Radiation-Induced Nucleation of Diamond from Amorphous Carbon: Effect of Hydrogen

6 AUTHORS, INCLUDING:

Alexander G. Kvashnin
Skolkovo Institute of Science and Technology
18 PUBLICATIONS **655** CITATIONS

Pavel Sorokin
Technological Institute for Superhard and N…
69 PUBLICATIONS **1,145** CITATIONS

W. Edward Billups
Rice University
237 PUBLICATIONS **6,244** CITATIONS

Radiation-Induced Nucleation of Diamond from Amorphous Carbon: Effect of Hydrogen

Yanqiu Sun,[†,‡] Alexander G. Kvashnin,[†,§,⊥,∥] Pavel B. Sorokin,[∥,⊥,#] Boris I. Yakobson,[†,§] and W. E. Billups*[,†,‡]

[†]Department of Chemistry, Rice University, 6100 Main Street, Houston, Texas 77005, United States

[‡]The Richard E. Smalley Institute for Nanoscale Science and Technology, Rice University, 6100 Main Street, Houston, Texas 77005, United States

[§]Department of Mechanical Engineering and Materials Science, Rice University, 6100 Main Street, Houston, Texas 77005, United States

[∥]Technological Institute for Superhard and Novel Carbon Materials, 7a Centralnaya Street, Troitsk, Moscow, Russia 142190

[⊥]Moscow Institute of Physics and Technology (State University), 9 Institutsky Lane, Dolgoprudny, Russia 141700

[#]Emanuel Institute of Biochemical Physics RAS, 4 Kosigin Street, Moscow, Russia 119334

ABSTRACT: Electron irradiation of anthracite functionalized by dodecyl groups leads to recrystallization of the carbon network into diamonds. The diamonds range in size from ∼2 to ∼10 nm and exhibit {111} spacing of 2.1 Å. A bulk process consistent with bias-enhanced nucleation is proposed in which the dodecyl group provides hydrogen during electron irradiation. Recrystallization into diamond occurs in the hydrogenated graphitic subsurface layers. Unfunctionalized anthracite could not be converted into diamond during electron irradiation. The dependence of the phase transition pressure on cluster size was estimated, and it was found that diamond particles with a radius up to 20 nm could be formed.

SECTION: Physical Processes in Nanomaterials and Nanostructures
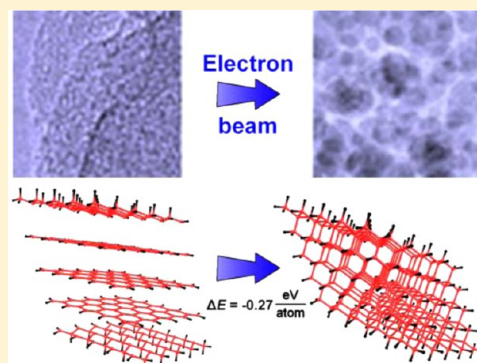
Chemical vapor deposition (CVD) of diamond has been developed so that diamond growth on diamond at subatmospheric pressure is efficient and well understood.[1] In contrast, diamond growth on nondiamond surfaces requires a nucleation step that has only recently been addressed.[2] Biased enhanced nucleation (BEN) has been shown to provide the most controlled pathway for nucleation onto nondiamond surfaces.[3,4] This process allows nucleation to be achieved either by direct ion beam bombardment[5] or by exposing a negatively biased substrate to a CVD plasma.[3,4] Nucleation sites that have been identified include the formation of randomly oriented diamond on graphite edges[6−8] and for heteroepitaxial oriented growth on silicon.[9]
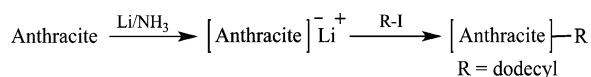
During our studies on the reductive alkylation of anthracite by dodecyl groups (Scheme 1),[10,11] we found that diamonds were formed when the dodecylated anthracite was exposed to the electron beam during analysis by transmission electron microscopy. Because extensive measurements with pristine anthracite failed to yield diamonds, we suggest that these results can be explained in terms of a process that is assisted by hydrogen atoms that are formed by the "knock-on" effect[12] from the hydrogen bearing dodecyl groups.

Nucleation would be an internal bulk process that occurs in subsurface layers, consistent with the model proposed and substantiated by Lifshitz and coworkers.[2] The layered structure of the unfunctionalized anthracite[11] is clearly visible in the transmission electron microscopy image shown in Figure 1a. The diamonds are embedded in amorphous carbon with fringes of ∼2.1 Å, corresponding to the {111} diamond crystal structure (Figure 1b). The diamond particles range in size from ∼2 to ∼10 nm. The high-resolution transmission electron microscopy images of anthracite reveal a layered structure with some regions that are amorphous and others with poorly orientated graphitic-like fringes.[11]
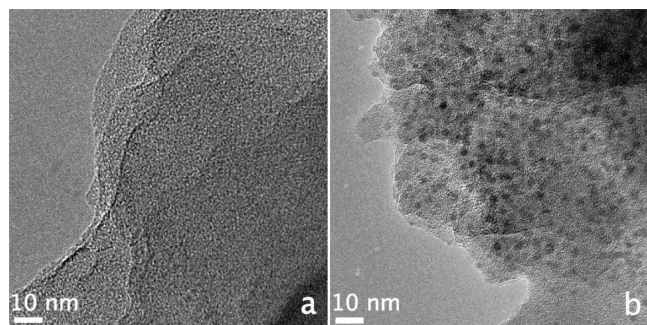
The bright-field high-resolution transmission electron microscopy images of a twinned diamond identified by the arrow in Figure 2a,b are shown more clearly in Figure 2c.

Scheme 1. Reductive Dodecylation of Anthracite.[10,11]

$$\text{Anthracite} \xrightarrow{\text{Li/NH}_3} \left[\text{Anthracite}\right]^{-}\text{Li}^{+} \xrightarrow{\text{R-I}} \left[\text{Anthracite}\right]\!-\!\text{R}$$
$$\text{R = dodecyl}$$

Figure 1. Bright-field high-resolution transmission electron microscopy images of (a) raw anthracite showing layers and (b) dodecylated anthracite showing diamonds (dark areas) after exposure to the 200 kV electron beam.

It is well known that the most stable carbon phase is graphite and that diamond is metastable. Although the energy difference between the two phases is only 0.01 to 0.04 eV/atom,[13,14] the high activation barrier (~0.4 eV/atom[15−17]) that is required to achieve the phase transition requires extreme conditions of temperature and pressure. However, on nanoscale the carbon phase diagram has to be reconsidered by introducing cluster size.[17−19] It has been shown recently that fullerenes are the most stable form of carbon for small clusters, while there is a "window" of stability for diamonds within the range 19−52 Å, beyond which graphite is more stable.[20,21] Small diamonds were observed to be unstable under electron irradiation.[22] We observed that electron irradiation of the particle shown in Figure 3a forms and then rapidly reforms the anthracite (Figure 3b−d). This transformation takes <30 s. The diameter of the diamond is ~2.5 nm.

The formation of diamond observed during this study is consistent with the model proposed and substantiated by Lifshitz and coworkers.[2] The graphitic-like layers of anthracite allow a bulk process to be initiated between the layers of the coal when hydrogen atoms displaced from the dodecyl groups by the "knock-on" effect[12] penetrate the anthracite and form a dense amorphous hydrogenated carbon (C:H) phase. After the carbon is saturated by hydrogen, precipitation of sp[3] carbon clusters would form. Most of the clusters would probably be amorphous, but a few would have the structure of diamond. The addition of hydrogen atoms to the dangling bonds would follow. The presence of hydrogen along the edges of the diamond would prevent the formation of the graphenic structure observed by Lueking and coworkers when anthracite was investigated as a vehicle for the storage of dihydrogen.[23,24] Ball milling of the anthracite with cyclohexene (the source of hydrogen) led to a carbon structure that decomposed upon
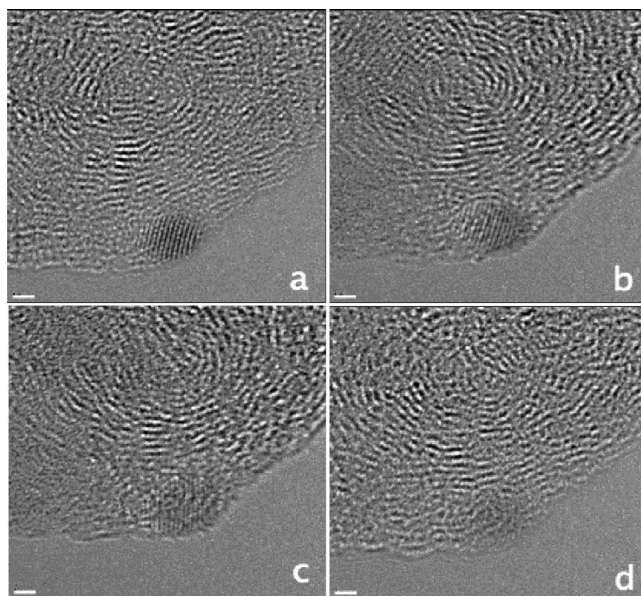

Figure 3. HRTEM images showing a nanodiamond reverting back to anthracite upon exposure to the electron beam. The scale bar is 1 nm.

heating to give molecular hydrogen. Crystalline regions were attributed to the high temperature (1400 °C) that was used to remove metals. The onion-like graphitic structures that surround the diamond probably formed when insufficient hydrogen was present to protect the edges of the diamond.

The elegant experiments that have been carried out recently by Dahl and his coworkers[25] emphasize the importance of hydrogen in the growth of diamondoids that occur naturally in oil. The lower members of this family have been synthesized through a series of carbocation rearrangements that eventually lead to the more stable lower homologues adamantane, diamantane, and triadamantane. Chemists have assumed logically that the large diamondoids that occur in high concentrations in oil are formed through similar rearrangements. However, these workers established a free radical process, similar to CVD growth, with hydrogen playing a dominant role. Similarly, recent studies have demonstrated that diamond nanowires can be formed inside carbon nanotubes with appropriate seeds in the presence of a hydrogen atmosphere.[26]

Experiments to demonstrate the importance of hydrogen were carried out by exposing the anthracite to a less robust source of hydrogen. Thus, when anthracite functionalized by n-butyl groups was exposed to the electron beam, regions were
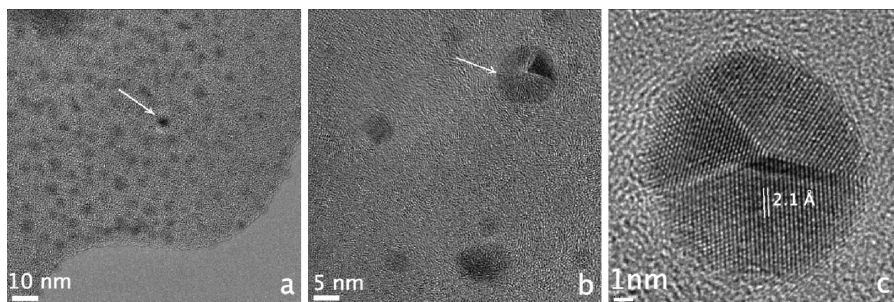
Figure 2. Bright-field high-resolution transmission electron microscopy images (a−c) of a single twinned diamond.

found where onion-like fringes started to form, but no fully formed diamonds could be observed (Figure 4).
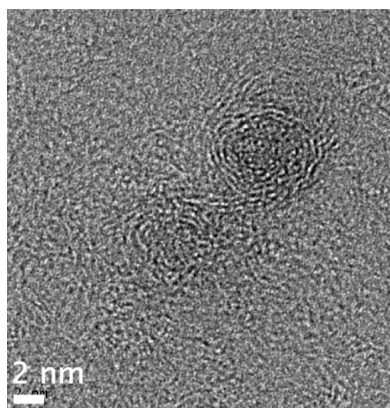
Figure 4. HRTEM image of anthracite functionalized by *n*-butyl groups showing changes in the amorphous carbon.

In contrast with anthracite,[10] reductive alkylation of subbituminous coal by dodecyl groups leads to a more complex mixture of products that result from collapse of the coal matrix during the reductive alkylation.[27] Despite the structural diversity of products, the HRTEM image of subbituminous coal functionalized by dodecyl groups shows nanoscale diamond particles distributed throughout the coal. When simple alkenes (dodecene) are grafted onto the coal, as described in our previous work,[27] an unusually high density of nanodiamonds is formed upon exposure of the polydodecene-grafted coal to the electron beam (Figure 5a,b). We attribute this observation to the high concentration of hydrogen atoms that are formed by irradiation of the hydrogen-rich polydodecene.
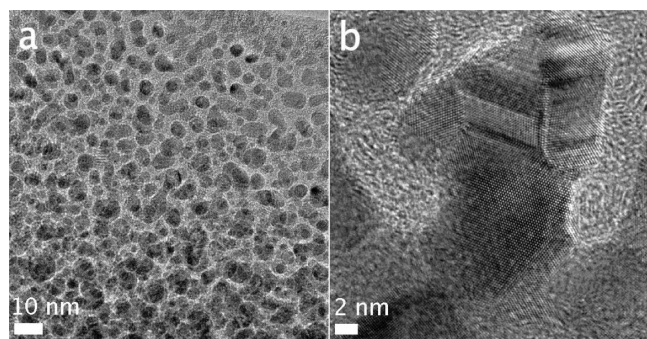
Figure 5. HRTEM images of nanodiamonds formed by electron irradiation of polydodecene-grafted subbituminous coal.

Other high-resolution images of nanodiamonds found in the polydodecene-grafted subbituminous coal after electron irradiation are illustrated in Figure 6a−c.

To substantiate the role of hydrogen in the formation of the diamond clusters, we used an atomistic simulation by reactive force-field potential (ReaxFF),[28] implemented in LAMMPS package.[29] To evaluate the accuracy of this approach, the corresponding characteristics of the bulk diamond were calculated using ReaxFF and compared with reference data. The phase-transition pressure (at 0 K) between graphite and diamond was evaluated as 4.76 GPa. This overestimates the

experimental value of graphite-diamond phase transition (1.7 GPa).[30]

Using graphene as a model, it was found that the adsorption of adatoms to a multilayered graphene surface leads to the formation of a diamond nanofilm without any activation barrier[17] (at least for the films containing two to six layers); this effect is termed a chemically induced phase transition. The experimental evidence of chemically induced phase transformations in carbon structures has been demonstrated for an amorphous structure[2] and for graphite[31] after exposure to either hydrogen or fluorine. In the latter case, X-ray, NMR, and electronic microscopy analyses[32] showed the formation of an ordered thin diamond film.

The binding of reference atoms to the surface of the layered carbon structure leads to the transformation of a nearly chemically inert sp^2-hybridized carbon lattice to a partially hydrogenated sp^3-hybridized structure. The dangling bonds not bound to hydrogen compensate by connecting to the underlying carbon layers to form the sp^3-hybridized structure. The carbon atoms that are not bound to hydrogen then form bonds to adjacent layers. This leads to a "zipping" process that results in the formation of sp^3-hybridized diamond without any activation barrier (at least for nanometer-sized objects).[17,33]

Because the diamond clusters that we observe have the (111) surface, a theoretical investigation was initiated using a model of diamondization of hydrogenated multilayered graphite clusters to diamond clusters faceted by (111) surfaces, as illustrated in Figure 7. The diamond clusters would be obtained from the hydrogenated multilayered graphene clusters by the formation of bonds between the neighboring layers.

We find that the graphene cluster with hydrogen bound to the surface has a binding energy that is less than the binding energy of the corresponding diamond cluster. Because this difference is negative, the formation of diamond will occur without an activation barrier.

Using atomistic simulation, the dependence of the phase-transition pressure upon the cluster radius was also calculated. (See Figure 8.) Using the method of Viecelli et al.,[18] the dependence of the phase transition pressure on the average cluster radius, compared with bulk diamond, could be fitted as $P(R) = -3934R^{-1} + 32\,866R^{-2} - 17\,899R^{-3} + 4.76$, where 4.76 GPa is the calculated phase-transition pressure of the diamond. It should be noted that for large clusters only the first term is sufficient. Therefore, the transition pressure is proportional to R^{-1}.

One can see from Figure 8 that the dependence of the phase-transition pressure on the average radius exhibits nonlinear behavior. The pressure increases with an increasing size of the cluster leading to the bulk value (4.76 GPa) and changes the sign (become positive) at >14 nm (Figure 8), which is in agreement with the experimentally observed range (2−10 nm). This result allows one to conclude that an activation barrier will appear only in the case of large clusters and that small particles will be obtained by chemical adsorption of hydrogen onto the carbon surface.

We should point out that the difference between the calculated data and the fit is related to nonspherical shapes of clusters. The average radii of the clusters could not be determined unambiguously by applying the analytical expression derived for spherical clusters. Also, the overestimation of phase-transition pressure could lead to the underestimation of the critical cluster size that would form under hydrogenation.
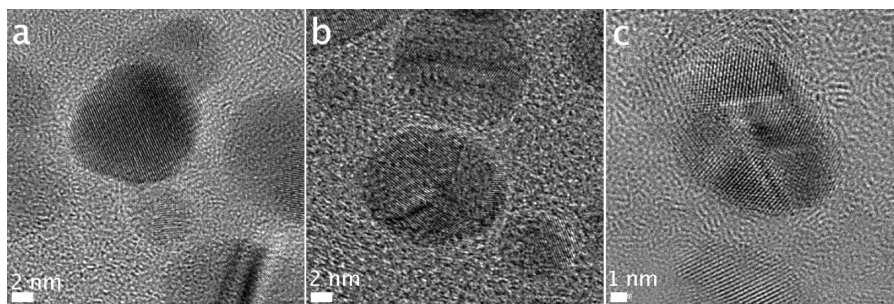
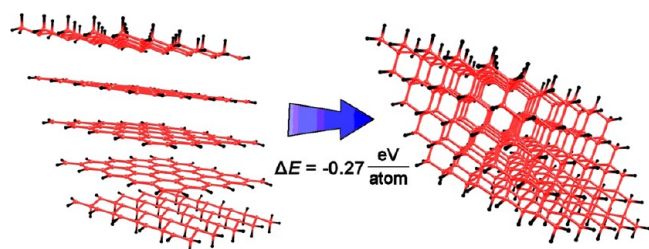**Figure 6.** Nanodiamonds found in polydodecene-grafted subbituminous coal after electron irradiation.

Figure 7. Atomic structure of five-layered graphene cluster with hydrogenated surface and corresponding diamond cluster. Hydrogen atoms are marked as black sticks.
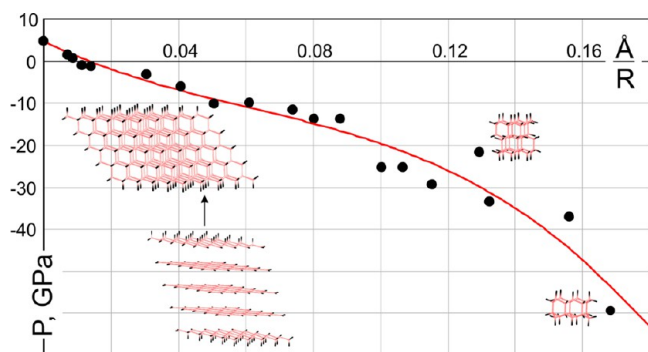

Figure 8. Dependence of phase-transition pressure on the inverse average radius of diamond clusters.

In conclusion, electron irradiation of either anthracite or a subbituminous coal functionalized by hydrogen-bearing groups leads to rearrangement of amorphous carbon into diamond. Consistent with a previous study,[2] it is proposed that a dense amorphous hydrogenated carbon phase (C:H) is formed that is further reduced by hydrogen to form sp^3 carbon clusters that contain some diamond structures. Dangling bonds along the edges are removed by reaction with hydrogen. The theoretical investigation shows that the adsorption of hydrogen plays a major role in the formation of diamond from amorphous carbon. It was estimated that this effect is dominant for clusters with an average radius up to 20 nm, in good agreement with the experimental result. These results can be critically important in the synthesis of ultrasmall diamond particles and can stimulate further investigations of sp^3-hybridized carbon particles.

EXPERIMENTAL SECTION

A sample of anthracite was obtained from J. Crelling (Southern Illinois University). The anthracite came from the Mammoth seam that is located in Schuylkill county Pennsylvania. The composition of the sample was determined by XPS to be 92% carbon and 6.4% oxygen. Nitrogen, silicon, and sulfur were each

present in <1%. Subbituminous coal came from Western Energy Company's Rosebud Mine in Montana. All other reagents were purchased from Aldrich. Both coals functionalized by dodecyl groups have been characterized fully during our previous studies.

HRTEM images were recorded using a JEOL 2100 field-emission transmission electron microscope (JEM 2100F TEM) operated at an accelerating voltage of 200 kV.

■ AUTHOR INFORMATION

Corresponding Author
*Tel: 713-348-5694. E-mail: billups@rice.edu.

Notes
The authors declare no competing financial interest.

■ REFERENCES

(1) Bundy, F. P.; Hall, H. T.; Strong, H. M.; Wentorf jun, R. H. Man-Made Diamonds. *Nature* **1955**, *176*, 51−55.

(2) Lifshitz, Y.; Kohler, T.; Frauenheim, T.; Guzmann, I.; Hoffman, A.; Zhang, R. Q.; Zhou, X. T.; Lee, S. T. The Mechanism of Diamond Nucleation from Energetic Species. *Science* **2002**, *297*, 1531−1533.

(3) Yugo, S.; Kanai, T.; Kimura, T.; Muto, T. Generation of Diamond Nuclei by Electric Field in Plasma Chemical Vapor Deposition. *Appl. Phys. Lett.* **1991**, *58*, 1036−1038.

(4) Jiang, X.; Klages, C.; Zachai, R.; Hartweg, M.; Füsser, H. Epitaxial Diamond Thin Films on (001) Silicon Substrates. *Appl. Phys. Lett.* **1993**, *62*, 3438−3440.

(5) Zhang, W. J.; Sun, X. S.; Peng, H. Y.; Wang, N.; Lee, C. S.; Bello, I.; Lee, S. T. Diamond Nucleation Enhancement by Direct Low-Energy Ion-Beam Deposition. *Phys. Rev. B* **2000**, *61*, 5579−5586.

(6) García, M. M.; Jiménez, I.; Vázquez, L.; Gómez-Aleixandre, C.; Albella, J. M.; Sánchez, O.; Terminello, L. J.; Himpsel, F. J. X-ray Absorption Spectroscopy and Atomic Force Microscopy Study of Bias-Enhanced Nucleation of Diamond Films. *Appl. Phys. Lett.* **1998**, *72*, 2105−2107.

(7) Hoffman, A.; Heiman, A.; Christiansen, S. H. Mechanism of Nanodiamond Film Formation by Stress Relaxation on a Preferentially Oriented Vertical Basal Plane Graphitic Precursor. *J. Appl. Phys.* **2001**, *89*, 5769−5774.

(8) Lambrecht, W. R. L.; Lee, C. H.; Segall, B.; Angus, J. C.; LI, Z.; Sunkara, M. Diamond Nucleation by Hydrogenation of the Edges of Graphitic Precursors. *Nature* **1993**, *364*, 607−610.

(9) Lee, S. T.; Peng, H. Y.; Zhou, X. T.; Wang, N.; Lee, C. S.; Bello, I.; Lifshitz, Y. A Nucleation Site and Mechanism Leading to Epitaxial Growth of Diamond Films. *Science* **2000**, *287*, 104−106.

(10) Sun, Y.; Kuznetsov, O.; Alemany, L.; Billups, W. E. Reductive Alkylation of Anthracite: Edge Functionalization. *Energy Fuels* **2011**, *25*, 3997−4005.

(11) Sun, Y.; Alemany, L. B.; Billups, W. E.; Lu, J.; Yakobson, B. I. Structural Dislocations in Anthracite. *J. Phys. Chem. Lett.* **2011**, *2*, 2521−2524.

(12) Krueger, A. The Structure and Reactivity of Nanoscale Diamond. *J. Mater. Chem.* **2008**, *18*, 1485−1492.

(13) Yin, M. T.; Cohen, M. L. Structural Theory of Graphite and Graphitic Silicon. *Phys. Rev. B* **1984**, *29*, 6996.

(14) Tateyama, Y.; Ogitsu, T.; Kusakabe, K.; Tsuneyuki, S. Constant-Pressure First-Principles Studies on the Transition States of the Graphite-Diamond Transformation. *Phys. Rev. B* **1996**, *54*, 14994−15001.

(15) Fahy, S.; Louie, S. G.; Cohen, M. L. Pseudopotential Total-Energy Study of the Transition from Rhombohedral Graphite to Diamond. *Phys. Rev. B* **1986**, *34*, 1191−1199.

(16) Furthmüller, J.; Hafner, J.; Kresse, G. Ab Initio Calculation of the Structural and Electronic Properties of Carbon and Boron Nitride Using Ultrasoft Pseudopotentials. *Phys. Rev. B* **1994**, *50*, 15606−15622.

(17) Kvashnin, A. G.; Chernozatonskiin, L. A.; Yakobson, B.; Sorokin, P. B. Phase Diagram of Quasi-Two-Dimensional Carbon, From Graphene to Diamond. *Nano Lett.* **2014**, *14*, 676−681.

(18) Viecelli, J. A.; Bastea, S.; Glosli, J. N.; Ree, F. H. Phase Transformations of Nanometer Size Carbon Particles in Shocked Hydrocarbons and Explosives. *J. Chem. Phys.* **2001**, *115*, 2730.

(19) Viecelli, J.; Ree, F. H. Carbon Particle Phase Transformation Kinetics in Detonation Waves. *J. Appl. Phys.* **2000**, *88*, 683−690.

(20) Barnard, A. S.; Russo, S. P.; Snook, I. K. Size Dependent Phase Stability of Carbon Nanoparticles: Nanodiamond Versus Fullerenes. *J. Chem. Phys.* **2003**, *118*, 5094−5098.

(21) Raty, J. Y.; Galli, G.; Bostedt, C.; Buuren, T. W. V.; Terminello, L. J. Quantum Confinement and Fullerenelike Surface Reconstructions in Nanodiamonds. *Phys. Rev. Lett.* **2003**, *90*, 037401.

(22) Mykhaylyk, O. O.; Solonin, Y. M.; Batchelder, D. N.; Brydson, R. Transformation of Nanodiamond into Carbon Onions: A Comparative Study by High-Resolution Transmission Electron Microscopy, Electron Energy-Loss Spectroscopy, X-ray Diffraction, Small-Angle X-ray Scattering, and Ultraviolet Raman Spectroscopy. *J. Appl. Phys.* **2005**, *97*, 074302.

(23) Lueking, A. D.; Gutierrez, H. R.; Fonseca, D. A.; Narayanan, D. L.; Van Essendelft, D.; Jain, P.; Clifford, C. E. B. Combined Hydrogen Production and Storage with Subsequent Carbon Crystallization. *J. Am. Chem. Soc.* **2006**, *128*, 7758−7760.

(24) Lueking, A. D.; Gutierrez, H. R.; Jain, P.; Essandelft, D. T. V.; Burgess-Clifford, C. E. The Effect of HCl and NaOH Treatment on Structural Transformations in a Ball-Milled Anthracite After Thermal and Chemical Processing. *Carbon* **2007**, *45*, 2297−2306.

(25) Dahl, J. E. P.; Moldowan, J. M.; Wei, Z.; Lipton, P. A.; Denisevich, P.; Gat, R.; Liu, S.; Schreiner, P. R.; Carlson, R. M. K. Synthesis of Higher Diamondoids and Implications for Their Formation in Petroleum. *Angew. Chem., Int. Ed.* **2010**, *49*, 9881−9885.

(26) Zhang, J.; Zhu, Z.; Feng, Y.; Ishiwata, H.; Miyata, Y.; Kitaura, R.; Dahl, J. E. P.; Carlson, R. M. K.; Fokina, N. A.; Schreiner, P. R.; Tománek, D..; Shinohara, H. Evidence of Diamond Nanowires Formed Inside Carbon Nanotubes from Diamantane Dicarboxylic Acid. *Angew. Chem., Int. Ed.* **2013**, *52*, 3717−3721.

(27) Sun, Y.; Mukherjee, A.; Kuznetsov, O.; Thaner, R.; Alemany, L. B.; Billups, W. E. Functionalization by Reductive Alkylation and Mapping of a Subbituminous Coal by Energy Dispersive X-ray Spectroscopy. *Energy Fuels* **2011**, *25*, 1571−1577.

(28) van Duin, A. C. T.; Dasgupta, S.; Lorant, F.; Goddard, W. A., III. Reaxff: A Reactive Force Field for Hydrocarbons. *J. Phys. Chem. A* **2001**, *105*, 9396−9409.

(29) Plimpton, S. Fast Parallel Algorithms for Short-range Molecular Dynamics. *J. Comput. Phys.* **1995**, *117*, 1−19.

(30) Bundy, F.; Bassett, W.; Weathers, M.; Hemley, R.; Mao, H.; Goncharov, A. The Pressure-Temperature Phase and Transformation Diagram for Carbon; Updated Through 1994. *Carbon* **1996**, *34*, 141−153.

(31) Watanabe, N. Two Types of Graphite Fluorides,(CF)n and (C2F)n, and Discharge Characteristics and Mechanisms of Electrodes of (CF)n and (C2F)n in Lithium Batteries. *Solid State Ionics* **1980**, *1*, 87−110.

(32) Touhara, H.; Kadono, K.; Fujii, Y.; Watanabe, N. On the Structure of Graphite Fluoride. *Z. Anorg. Allg. Chem.* **1987**, *544*, 7−20.

(33) Kvashnin, A. G.; Sorokin, P. B. Lonsdaleite Films with Nanometer Thickness. *J. Phys. Chem. Lett.* **2014**, *5*, 541−548.

1928

dx.doi.org/10.1021/jz5007912 | *J. Phys. Chem. Lett.* 2014, 5, 1924−1928